An Experimental Study on the Inelastic Behavior of Steel Frames Subjected to Vertical and Horizontal Loading

AUTHOR(S):

WAKABAYASHI, Minoru; NONAKA, Taijiro; MATSUI, Chiaki

Bull. Disas. Prev. Res. Inst. Kyoto Univ., Vol. 17, Part 1, No. 119, July, 1967

An Experimental Study on the Inelastic Behavior of Steel Frames Subjected to Vertical and Horizontal Loading

By Minoru WAKABAYASHI, Taijiro NONAKA
and Chiaki MATSUI

(Manuscript received May 30, 1967)

Abstract

An experimental study was made of the behavior of single bay, one- and two-storyed frames, using mild steel models with wide flange sections. A varying horizontal force was applied at the top of a frame model under a constant vertical load on the columns. From the horizontal force-displacement relation, a considerable reduction was observed in the restoring force due to the column loads, indicating the importance of the unstable character due to dead loads on the horizontal restoring force in tall buildings.

In general the experimental results show more favourable behavior for a large deformation than the elastic-perfectly plastic theory predicts and a rough estimation of the strain-hardening effects accounts for this behavior in a reasonable way.

1. Introduction

Normal building structures are subjected to wind and earthquake forces as well as dead, live and snow loads. Usually the latter act vertically and more or less constantly, while the former basically act in a horizontal direction and vary with time and space. Hence the strength of a structure hinges, among other things, on the behavior of the structural frame under constant vertical loads and varying horizontal forces. The existence of vertical loads somehow induces the unstable feature of a structure.[1)-3)]* The development of the plastic analysis of structures facilitates clarification of the ultimate state or the real strength of a structure. It normally neglects the instability effect of vertical loads. The destabilizing phenomenon, however, becomes more important as the structure gets higher, so that the vertical loads increase. This phenomenon is also significant when the horizontal displacement is large, even if vertical loads are small.

In modern multi-story frames, structural members are getting slender because of the adoption of high-strength steel and this also makes destabilizing phenomena important in structural behavior.

A systematic study to investigate the behavior of a structure under such conditions is imminent. It seems that no complete theoretical analysis is available, owing to computational difficulties.[4)] Plenty of tests have been carried out to check the validity of the plastic analysis of structures,[5)-8)] but they have been mostly carried out in conditions where vertical loads are either absent or so

* Numbers with parenthesis refer to the bibliography at the end of the paper.

small that they have no significant effect on the overall response or the unstable character of frame behavior. The results of these tests, therefore, can not be directly applied to multi-story frames.

Prior to the experiment reported here, a series of preliminary tests was performed using miniature steel models of a portal frame with rectangular cross sections.[9),10)] The destabilizing phenomena of the frame models were clearly observed in the horizontal force-displacement curves. During the preparation of the present paper, the authors' attention was drawn to a paper[11)] by Makino, Sato and Miyazaki, and a paper[12)] by Arnold, Adams and Lu. In the former, a study was made in order to check on the applicability of the plastic hinge method to a rigid frame under constant vertical and horizontal repeated forces. It consists of results of a test on steel models with a rectangular cross-section. Some models indicated a negative slope in the horizontal force-displacement curve. The latter paper is concerned with results of a test on a single story, single bay, hybrid frame with full scale, wide flange sections. It claims that high strength steel can be used with confidence for structural frames and that the behavior of high strength members can be predicted by methods conventionally used for structural carbon steel members. The authors' group has conducted several tests along similar lines, using mild steel models of rectangular cross sections for one bay, three and five story frames.[13)]

In this paper, the experimental results for one and two story portal frames with wide flange sections will be described. Vertical loads are applied constantly on the columns, and a varying horizontal force was applied at top floor level. A theoretical analysis was made so as to study the elastic-plastic behavior of the frames for comparison with the experimental results. We attempted to include the strain-hardening effects in the inelastic range in an approximate way, in order to gain access to the real behavior of the frames tested.

2. Description of the Tests

2. 1 Object and Scope of the Tests

The behavior of a steel multi-story frame under a varying horizontal load was experimentally studied, using approximately 1/4-scale models. The main influential factors on the behavior of frames are, among others, 1° the number of stories and bays, 2° the magnitude of the vertical loads on the frame, 3° the slenderness of the columns, 4° the relative stiffness of the columns and beams, 5° the shape of the cross-sections of the members, 6° the mechanical properties of the materials, 7° the existence of residual stresses, etc.

In this experiment, special attention was paid to the effects of the axial forces existing in the columns on the behavior of unbraced steel frames. The effects of the conditions 1°, 2°, 4°, and 7° were also investigated. The test program consisted of eight specimens of one-bay rectangular frames, and was composed of two series, each containing four specimens: Series I for one story frames and Series II for two story. The test frames and their loading condition are shown for Series I and II in Figs. 1 (a) and 1 (b), respectively. Constant vertical loads are applied symmetrically at the top of the upper columns by an oil-pressere testing machine. Horizontal force was applied to the beam-to-column connection of the upper story by an oil jack. The magnitude of the vertical loads

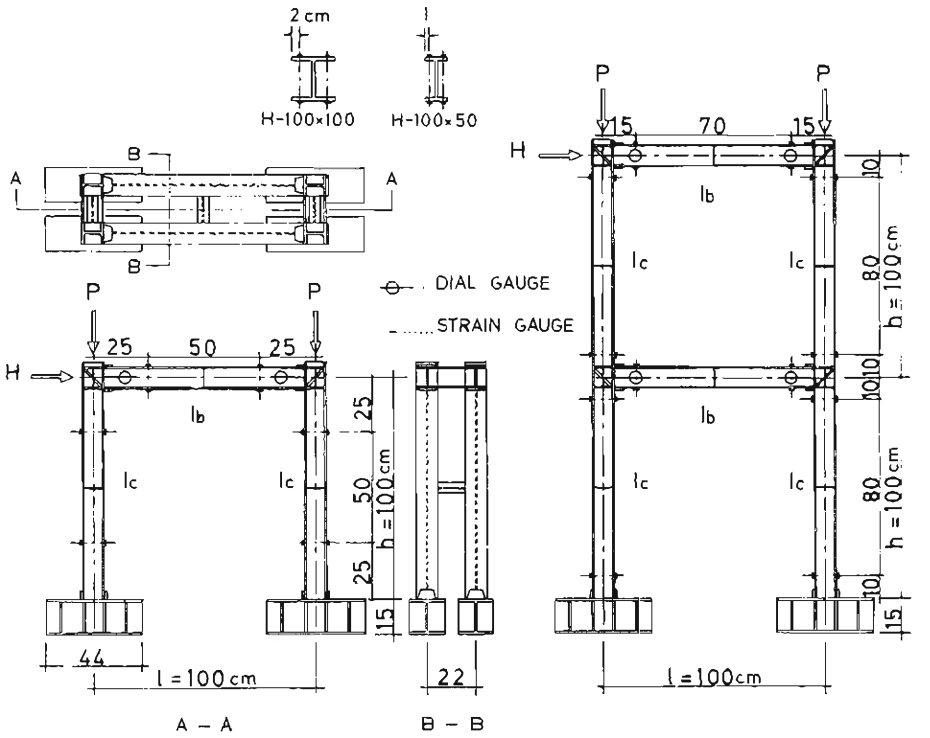

(a) Series I (b) Series II

Fig. 1. Test Frames.

was decided so that it had approximately the same proportion to the yield load of the columns as in a lower story of an actual multi-story frame in this country** but the loading condition given in this experiment was somewhat different from the actual situation. In an actual multi-story frame vertical loads are applied on the beam members as well as on the columns. Wind load is distributed over the height of a building and earthquake force does not act only on the top floor. However, the fundamental characteristics of these situations will be depicted in the behavior of the frame under the loading conditions in Fig. 1.

2. 2 Test Frames and Material Properties

Test frames were made by welding beams and columns of mild steel wide-flange sections and were designed to the dimensions shown in Table 1. Most actual frames in Japan have beam-to-column stiffness ratios in the range of those given here. The ratio of column height to the radius of gyration is also the representative value of multi-story frames. In order to prevent out-of-plane

** The ratio of the vertical load P to the elastic buckling load P_n of a frame is shown in Table 5. The ratio varies from 2 to 7 %; the tangent modulus buckling load is not much different from the yield load P_y. The frames are rather stubby, as compared with frames mostly used in foreign countries.

TABLE 1.
Nominal Dimensions of Test Frames.

Specimen number	P (ton)	h/i	Column (mm)	Beam (mm)	$I_b \times h/(I_c \times l)$	Heat treatment
I—1	20	24	H-100×100×6×8	H-100×50×4×6	0.43	none
I—2	〃	〃	〃	〃	〃	annealed
I—3	〃	〃	〃	H-100×100×6×8	1.00	none
I—4	〃	〃	〃	〃	〃	annealed
II—1	10	24	H-100×100×6×8	H-100×50×4×6	0.43	none
II—2	20	〃	〃	〃	〃	〃
II—3	10	〃	〃	H-100×100×6×8	1.00	〃
II—4	20	〃	〃	〃	〃	〃

P: column load h: column height l: beam length
i: radius of gyration of a column for in-plane flexure
I: sectional moment of inertia
$I_b \times h/(I_c \times l)$: beam-to-column stiffness ratio
Subscripts c and b stands for the column and beam, respectively.

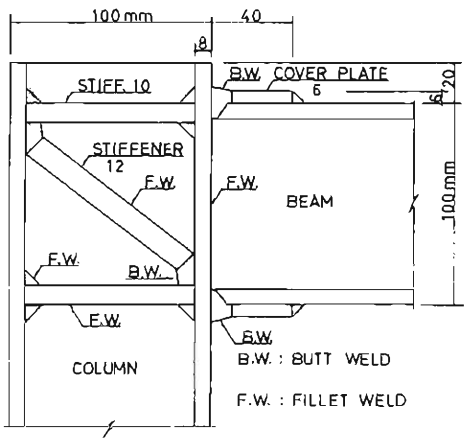

Fig. 2. Beam-to-Column Connection.

deformation, two identical plane frames were connected parallel to each other, to form a specimen, by welding a piece of wide flange section at several points across the two frames. The connection and the bottom ends of the columns were stiffened by welding cover plates and stiffeners as shown in Figs. 1 and 2. This was to prevent local failure at these parts before the overall collapse of the frame. The column feet were welded to large wide flange sections so as to fix the specimen rigidly on the supporting frame. Specimens I-2 and I-4 were annealed after they were constructed.

The actual section dimensions of each frame member were measured at both ends and in the center with micrometer and callipers. The length of the members was measured with steel measuring tape. Average values of the measurements were used for the analysis and are shown in Table 2. Table 3 shows the section properties of each test frame calculated from the values in Table 2. The effect of the rounded corners of a wide flange section at the flange-and-web connections is taken into account, since it turns out that the effect goes up to four per cent on the section properties.

Tensile test specimens were taken from a flange of one of the stock wide-flanges with which the test frames were made, as shown in Fig. 3. They were tested by an oil pressure testing machine with a capacity of 30 tons. The material properties were observed for each frame member, as shown in Table

4. A typical stress-strain relation is shown for a specimen without annealing in Fig. 4.

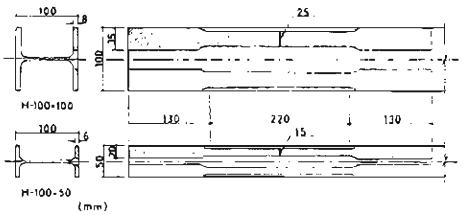

Fig. 3. Tensile-Test Specimen (Unit : mm)

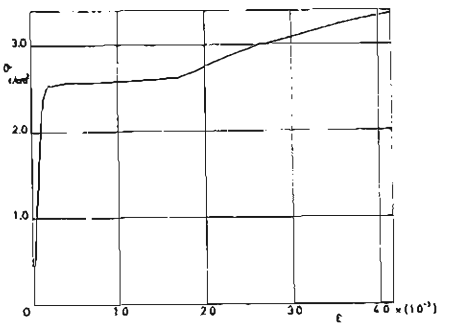

Fig. 4. Stress-Strain Relation (No Heat-Treatment).

TABLE 2.
Actual Dimensions of Test Frames.

Specimen number	h (cm)	l (cm)	Column D (cm)	Column B (cm)	Column t_w (cm)	Column t_f (cm)	Beam D (cm)	Beam B (cm)	Beam t_w (cm)	Beam t_f (cm)
I—1	100.02	100.04	10.106	10.028	0.679	0.765	10.164	5.004	0.465	0.643
I—2	99.97	99.94	10.095	10.034	0.685	0.772	10.165	4.993	0.460	0.645
I—3	99.84	100.09	10.154	10.062	0.693	0.814	10.165	10.063	0.698	0.811
I—4	99.87	99.85	10.147	10.066	0.694	0.809	10.155	10.052	0.694	0.811
II—1	99.87	98.75	10.103	10.026	0.584	0.799	10.140	5.001	0.420	0.645
II—2	99.86	99.64	10.133	9.987	0.592	0.812	10.133	5.002	0.419	0.645
II—3	100.30	99.63	10.098	10.021	0.593	0.803	10.120	9.990	0.591	0.814
II—4	99.87	99.75	10.114	9.981	0.609	0.812	10.128	10.020	0.597	0.807

D : depth of section B : width of section
t_w : thickness of web t_f : thickness of flange

TABLE 3.
Actual Section Properties of Test Frames.

Specimen number	Column A (cm²)	Column I (cm⁴)	Column Z (cm³)	Column Z_p (cm³)	Beam A (cm²)	Beam I (cm⁴)	Beam Z (cm³)	Beam Z_p (cm³)	$\frac{I_b \times h}{I_c \times l}$
I—1	22.04	385.2	76.23	87.55	11.12	184.5	36.30	42.45	0.479
I—2	22.22	387.2	76.70	88.15	10.98	183.1	36.02	42.37	0.473
I—3	23.17	408.1	80.38	92.50	23.17	408.5	80.37	92.48	1.000
I—4	23.08	406.0	80.03	92.07	23.12	406.8	80.11	92.22	1.000
II—1	21.88	391.7	77.53	88.61	10.80	181.2	35.74	41.51	0.463
II—2	22.15	396.9	78.33	87.72	10.70	181.1	35.75	41.50	0.456
II—3	22.02	392.9	77.81	88.90	22.17	397.7	78.60	89.74	1.012
II—4	22.27	396.7	78.45	89.78	22.21	396.9	78.38	89.60	1.000

A : cross-sectional area Z : section modulus Z_p : plastic section modulus

TABLE 4.
Material Properties of Test Frames.

Specimen number	Column				Beam			
	σ_y (t/cm^2)	σ_u (t/cm^2)	ε_u (%)	M_o (t·cm)	σ_y (t/cm^2)	σ_u (t/cm^2)	ε_u (%)	M_o (t·cm)
I—1	2.92	4.55	26.5	255.65	3.54	4.72	25.0	150.27
I—2	2.90	4.52	26.0	256.80	3.44	4.63	20.2	145.75
I—3	2.98	4.75	24.3	275.65	2.98	4.74	24.3	275.59
I—4	2.86	4.63	26.2	263.32	2.86	4.63	26.2	263.75
II—1	2.64	4.22	28.3	233.92	3.04	4.27	20.1	126.18
II—2	2.67	4.21	28.9	239.55	3.08	4.40	20.1	127.81
II—3	2.73	4.31	28.2	242.70	2.63	4.23	28.4	236.03
II—4	2.73	4.26	28.3	245.09	2.73	4.26	28.6	244.62

σ_y: yield point stress σ_u: tensile strength
ε_u: maximum elongation M_o: full plastic moment in pure bending

2. 3 *Loading Arrangement*

The experimental arrangement is shown in Fig. 5 and Photo. 1. The test

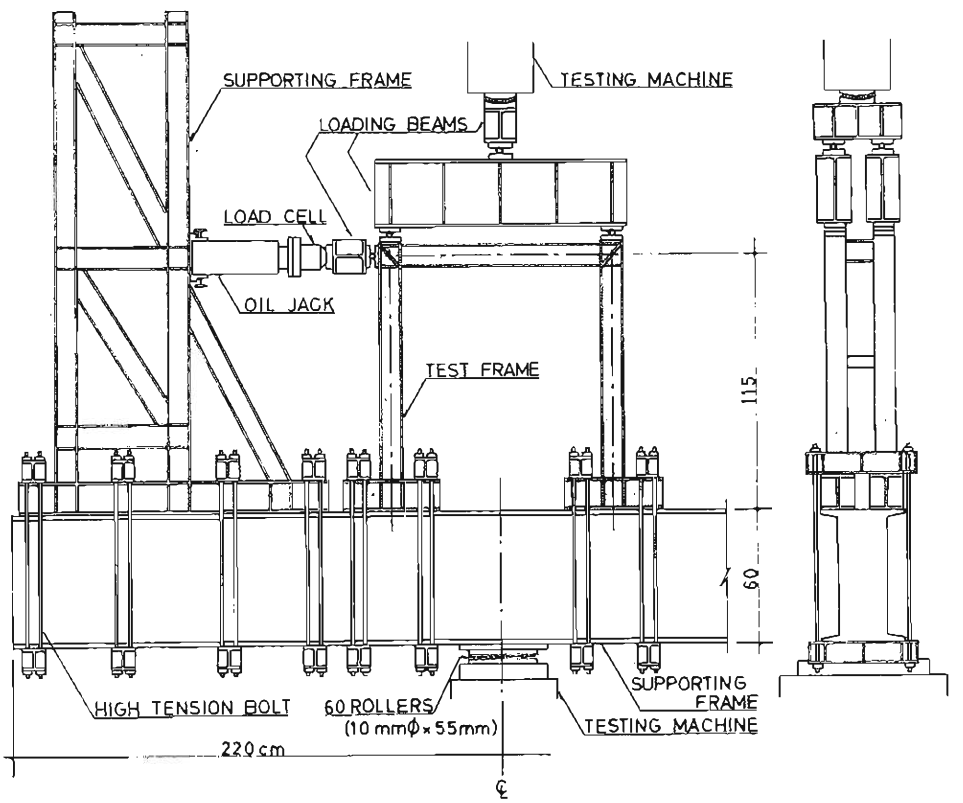

Fig. 5. Loading Arrangement.

specimen was fixed on the L-shape supporting frame at the foot of the lower columns through 16 high-tension bolts, Photo. 2. The supporting frame was set on an oil pressure testing machine with 100 ton capacity. Rollers were placed between the supporting frame and the testing machine bed, in order to allow the supporting frame to move horizontally, Photo. 3. The vertical load supplied by the testing machine is distributed equally among the tops of the four upper columns, Photo. 4. Horizontal force was applied by an oil jack with a capacity of 50 tons which was fixed on the supporting frame, Photo. 5, and was also distributed equally between the two frames of the specimen at the upper beam-to-column connections.

The friction of the rollers was examined experimentally, prior to the tests reported here. A similar arrangement of the rollers was set up. A vertical load was applied and the magnitude was changed up to the maximum load given in the tests. The horizontal force necessary to cause a small horizontal displacement against the friction of the rollers at each vertical loading step was measured. It was observed that the horizontal force was nearly proportional to the vertical load, the ratio being approximately 4/1000.

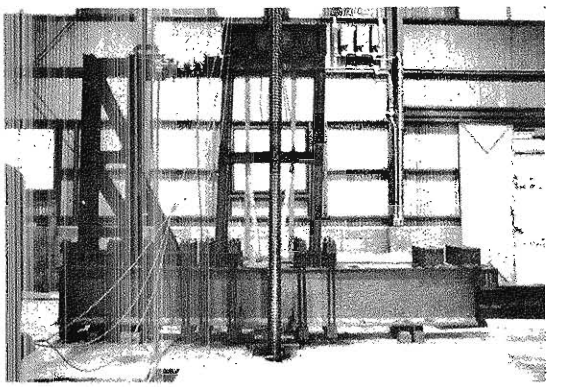

(a)

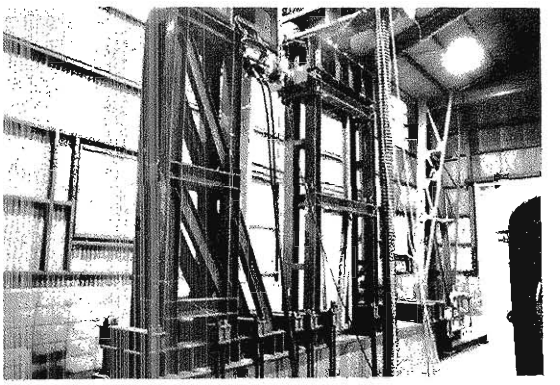

(b)

Photo. 1. Experimental Apparatus.

Photo. 2. Fixing at Column End.

As to the loading process, the vertical load was first set to the assigned value, and then the horizontal force was continuously varied in a quasi-static manner. The vertical load was maintained at the assigned value during the test by controlling the oil pressure. The horizontal force was slowly removed after

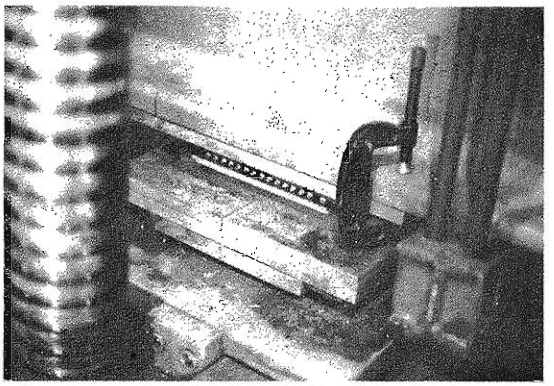

Photo. 3. Rollers.

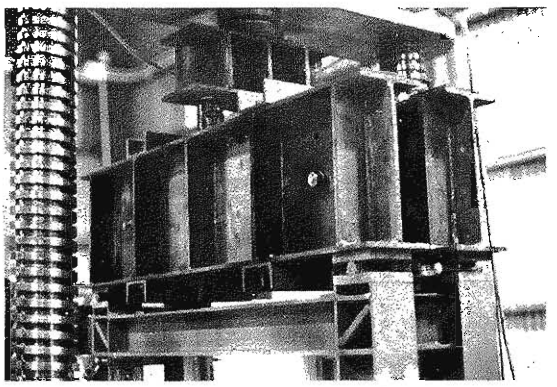

Photo. 4. Vertical Loading System.

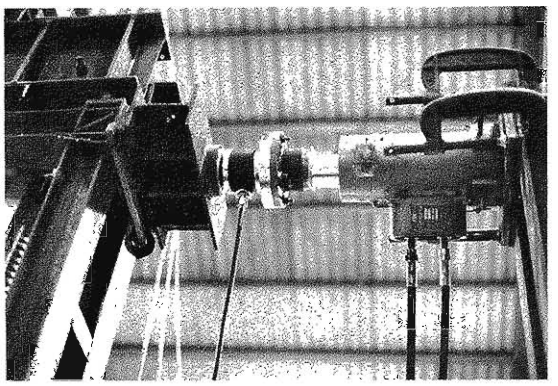

Photo. 5. Horizontal Loading System.

attainment of an angular displacement of about 0.04~0.06 radians with respect to the column feet. It was carefully checked that no appreciable horizontal displacement took place before horizontal load application.

2. 4 Instrumentation

The vertical load applied to the tops of the columns was measured by an oil pressure dial on the testing machine. The horizontal load was measured by a load cell placed between the oil jack and the specimen. The horizontal relative displacements between the stories were measured by means of dial gauges with 1/100mm scale, Fig. 1, and the strains were measured by wire strain gauges at the points also shown in Fig. 1.

2. 5 Experimental Observations

The behavior of the frames observed is shown in Figs. 14 and 15. The dimensionless horizontal load was taken for the ordinate, and the dimensionless displacement for the abscissa. The vertical load was set to an assigned value after eight loading steps. The deformation of the frame was observed at each loading step. The horizontal displacement at upper floor level was, at maximum, 3/10,000 times the frame height, before horizontal load application. The horizontal loading step is clear from Figs. 14 and 15. The hollow circles designate the experimental values.

In the elastic range of the strain measurements, the axial force of the columns was calculated from the strains. This was compared with the given vertical load which the testing machine dial indicated. The former was in the range of

94 to 104 % in Series I and 85 to 95 % in Series II, of the latter. The dial readings are used in the following analysis. The horizontal force was also calculated on the basis of the strain measurements in the columns. The bending moment distribution was known from the strains, and the column shears were found from the bending moments and the overturning moment due to the axial force of the columns; the horizontal load should be equal to the sum of the shears in left and right columns in an ideal situation. The calculated horizontal load was in the range of 90 to 100 % in Series I, and of 85 to 90 % in Series II, as compared with the load-cell readings. The friction force due

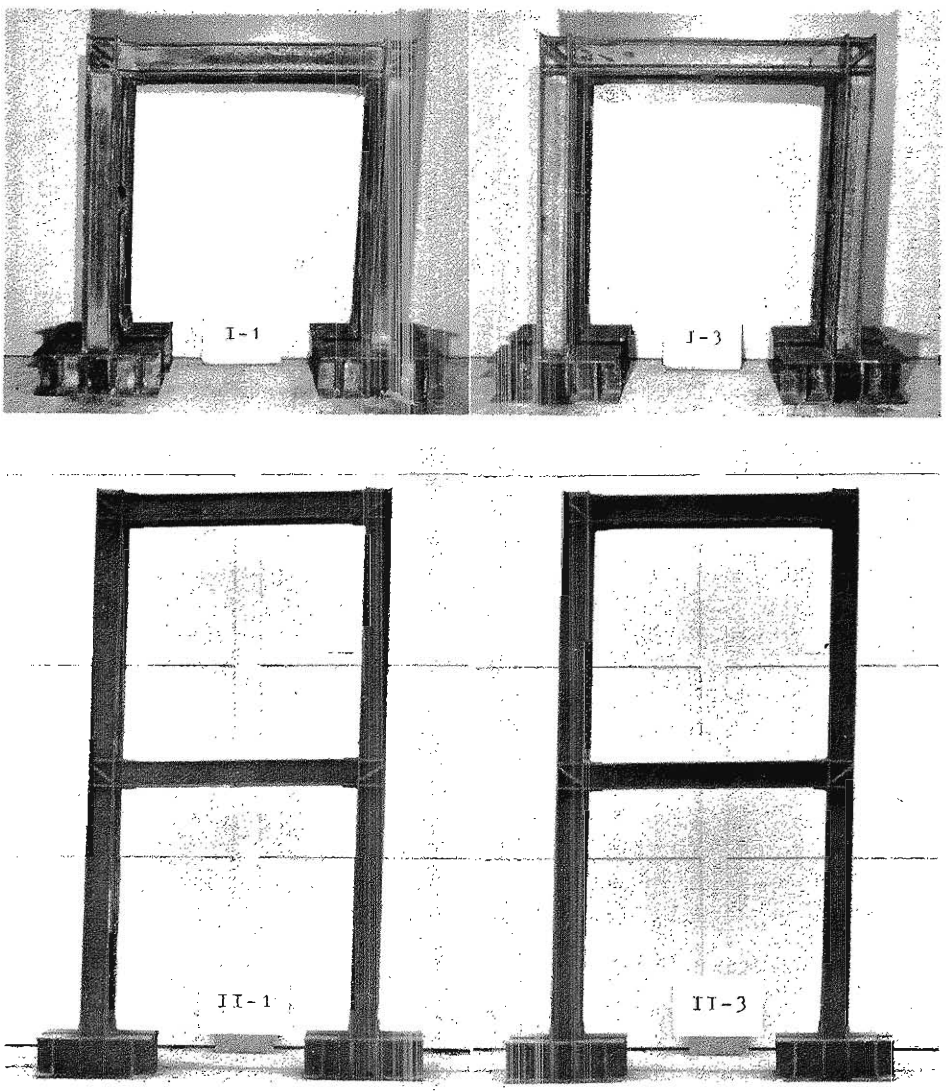

Photo. 6. Specimens after Test.

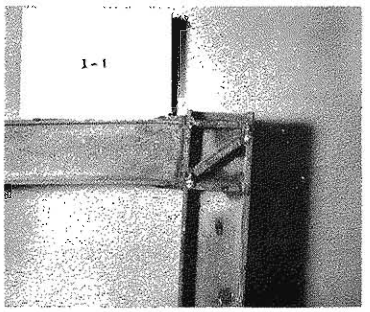

Photo. 7. Permanent Deformation at Beam End.

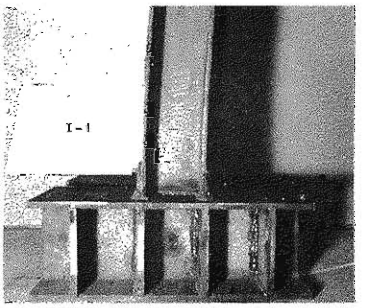

Photo. 8. Permanent Deformation at Column End (on the more severely compressed side).

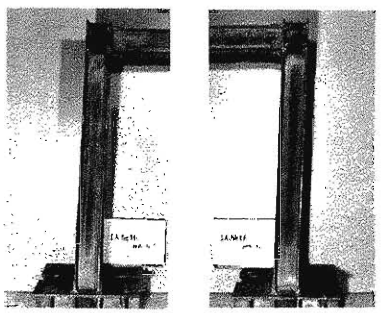

Photo. 9. Permanent Deformation in Columns.

to the rollers, placed at the frame base, could not be beyond 3.2%*** of the applied horizontal force, according to the 4/1,000 friction coefficient. The friction, therefore, does not fully compensate the difference. The cause may be mainly due to imperfect measurement of the strains, and we trusted the readings of the load cell.

Throughout the tests, no out-of-plane deformation nor local buckling phenomenon was observed. No appreciable deformation was observed at the beam-to-column connections. The strain measurements followed the process of critical sections yielding one after another. Observation of the order of yielding shows agreement with the formation of plastic hinges in the theoretical prediction (see Fig. 8).

A typical permanent deformation is seen in Photo. 6. The pictures were taken after the test. The beams remain straight except for small regions at the ends where the permanent deformation is concentrated; in columns the deformation is distributed over a wider range near their ends, Photos. 7 and 8. This is attributed to the axial forces in the columns. It can be observed that the curvature is more pronounced in the columns on the side where the beam shear increases the column axial forces than in the columns on the other side, Photo. 9. All the frame specimens show configurations in which large plastic deformation has taken place at the member ends in accordance with the locations of plastic hinges (compare Photo. 6 with Fig. 8).

3. Theoretical Analysis

In order to determine the restoring-force characteristics, or the horizontal force-displacement relation under the constant vertical load, we first make the following assumptions:

*** This corresponds to that of Specimen number II-2.

1° The frame is composed of one dimensional members.

2° Although geometry change is considered, the deflections are so small that the cosine of the slope angle can be approximated as unity, and load directions are preserved.

3° Members are subject to flexural deformation only, the axial and shearing deformation being negligible.

4° The moment-curvature relation is elastic-perfectly plastic until a sufficient number of sections reach the full plastic state so that the frame is reduced to a kinematic mechanism according to the theory of perfect plasticity (We shall now call it the mechanism state).

5° The interaction of the moment and the axial force is considered for the fully plastic condition of the columns, the effect of shear being ignored.

6° The effects of the axial force and the shear in the beams on the full plastic condition and on the bending stiffness are negligible.

7° No out-of-plane deformation nor any local buckling phenomena occur.

8° Effects of the residual stresses are negligible for the deformation characteristics of the frame.

When the loads are so small that the condition of linear elasticity is satisfied throughout the frame under consideration, the problem is solved by applying the slope-deflection method which takes care of the effect of the longitudinal force on the rigidity of a member. The fundamental slope-deflection equations are written, so far as no intermediate loads act, as

$$M_{AB}=\frac{2EI}{l}(\alpha\theta_A+\beta\theta_B-\gamma R)$$
$$M_{BA}=\frac{2EI}{l}(\alpha\theta_B+\beta\theta_A-\gamma R) \tag{1}$$

and

$$Q=\frac{-2EI}{l^2}(\gamma\theta_A+\gamma\theta_B-\delta R) \tag{2}$$

where the symbols, referring to the member AB, Fig. 6, are:

M_{AB}: the end moment at A
M_{BA}: the end moment at B
Q: the shear force
EI: the flexural rigidity
l: the length
θ_A: the slope angle at A
θ_B: the slope angle at B
R: the angular relative displacement between the ends
N: the axial compressive force

$$z=l\sqrt{\frac{N}{EI}}$$

$$\alpha=\frac{1}{2}\cdot\frac{z\sin z-z^2\cos z}{2(1-\cos z)-z\sin z}$$

$$\beta=\frac{1}{2}\cdot\frac{z^2-z\sin z}{2(1-\cos z)-z\sin z}$$

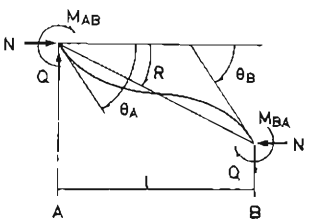

Fig. 6. Notations and Directions.

$$\gamma = \alpha + \beta$$

$$\delta = 2\gamma - \frac{z^2}{2}$$

The positive direction of the quantities are shown in the figure.

By applying Eq. (1) for the equilibrium condition of moment at each joint, and Eq. (2) for the equilibrium condition of the horizontal forces of each story, we get a sufficient number of equations for the unknown θ's and R's.

In order to take into account the variation of the axial forces of the columns due to the shear forces in the beams, we first assume the shear forces, and hence N's of the columns. The coefficients α, β, γ, δ are determined, and θ's and R's are found from the equilibrium conditions of the frame. The shear forces of the beams are then found from Eq. (2), N being set equal to zero. If the shear forces thus calculated are different from the assumed shear forces, a similar process is repeated using the shear forces obtained as the next trial values, until the necessary accuracy is acquired.

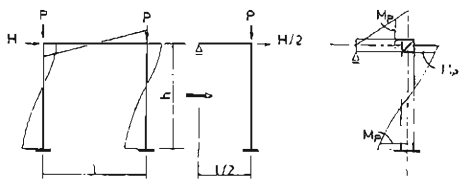

Fig. 7. Bending Moment Distribution.

When the variation of the axial forces is neglected, we only have to consider the right or the left half of the frame under consideration, taking account of the anti-symmetric property, as shown in Fig. 7 (a).**** The slope angle at the beam center is eliminated from Eq. (1), by setting the corresponding end moment equal to zero.

When the loads attain such a magnitude that a full plastic condition is satisfied at an end section of a member, forming a plastic hinge there, the appropriate end moment in Eq. (1) is set, in magnitude, to the full plastic moment of that member. By eliminating the corresponding θ from Eq. (1), we proceed to determine the elastic deformation of the rest of the frame, having again an equal number of unknowns and equilibrium conditions, until another section reaches the state of full plasticity. A similar process is continued up to the mechanism state. If we disregard the variation in the axial force of the columns, we can find the order of the formation of the plastic hinges without difficulty. It is shown for the right half of each specimen in Fig. 8.

The elastic-perfectly plastic type of analysis does not describe the realistic behavior of a steel frame, because actual steel shows some strain-hardening behavior in a large deformation range; the elastic-perfectly plastic analysis

**** Since the actual specimens are stiffened by cover plates at the member ends, a member is taken to have the fictitious full plastic moment which would occur at the member end (beam-to-column joint of the center lines), when the section at the end of the cover plate has the full plastic moment of that member, Fig. 7 (b). At the column ends where cover plates are absent, the fictitious full plastic moment is determined to be the one corresponding to the full plastic moment of the column at the end section of the connection panel.

does not agree very well with experimental results.[9),11)] Mild steel does not generally enter the strain-hardening range until a certain amount of plastic deformation occurs. The full plastic state is reached in several sections at different stages of loading. When a sufficient number of cross sections reach the full plastic state so that the frame would be reduced to a kinematic mechanism according to the perfect plasticity theory, the strain-hardening may have been experienced in the sections where the full plastic state is reached at an earlier stage. However, at sections where the full plastic state is reached at a later stage may not have entered the strain-hardening range. Therefore, we may take it that, on the average, the frame begins to suffer strain-hardening after the mechanism state. Thus, we assume:

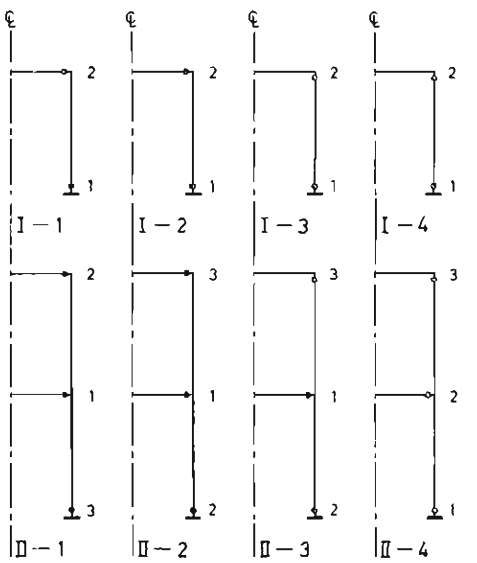

Fig. 8. Formation of Plastic Hinges.

9° The frame gets strain-hardened upon the arising of the mechanism state in the critical sections simultaneously; the incremental moment and the incremental curvature have a linear relationship.

For this assumption, it may be reasonable to take it that the factor τEI relating the incremental bending moment to the incremental curvature (Fig. 9) is based on the average slope in the inelastic range of the stress-strain relationship (Fig. 10), and we assume:

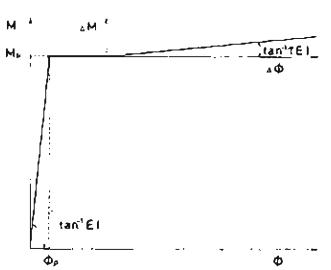

Fig. 9. Assumed Moment-Curvature Relation.

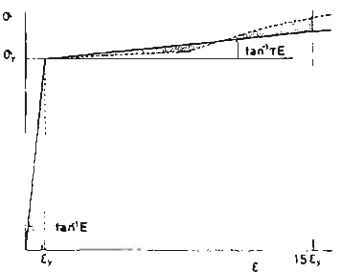

Fig. 10. Assumed Stress-Strain Relation.

10° $\tau = 1/100$

This is evaluated in such a way that the work done in the extension with a strain of 15 times the elastic limit strain is approximately the same in both the actual relation and the approximated bi-linear relation.

In order to simplify the calculation in the strain-hardening stage, we make the additional assumptions as follows:

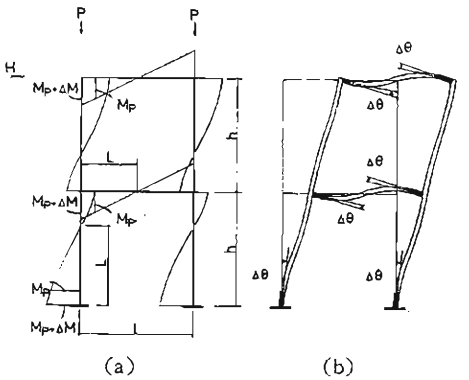

Fig. 11. Moment Distribution and Plastic Zones.

11° A plastic hinge spreads into a plastic zone in the member in which the full plastic state is reached, and it does not extend into the neighbouring members, Fig. 11.

12° The length of a plastic region is small in comparison with the length of the member, and the additional elastic deformation after the arising of the mechanism state is negligible.

13° The effect of the axial force on the incremental deformation of a column is negligible and the inflexion point does not change its position.

Let M_p denote the initial value of full plastic moment, the effect of the axial force being considered, and $M_p+\Delta M$ be the current full plastic moment. Considering the bending moment diagram, as in Fig. 11, we first establish the relationship between the moment $M_p+\Delta M$ applied at one end of a simply supported beam with span L and the end slope angle $\theta_p+\Delta\theta$, where θ_p is the end slope angle corresponding to the end moment M_p, Fig. 12. The incremental slope angle $\Delta\theta$ due to the purely plastic deformation is obtained, by applying, e.g., Mohr's principle, as

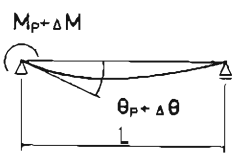

Fig. 12. Simply-Supported Beam Subjected to End Moment.

$$\frac{\Delta\theta}{\theta_p}=\frac{1}{2\tau}\cdot\frac{(\Delta M/M_p)^2}{(1+\Delta M/M_p)^2}\left(3+2\frac{\Delta M}{M_p}\right) \tag{3}$$

The relation is shown by a solid line in Fig. 13. This is for the case where a finite plastic zone arises near the end. We apply this relation to beams in Fig. 11 (a) with $L=l/2$. We also apply the relation to the columns based on the assumption 13°. L is taken to be the distance between the end and the inflexion point, which is assumed to remain at the position where it was at the mechanism state. Noting that the incremental end angle $\Delta\theta$ is the same both for the beams and for the columns based on the assumption 12°, we find the horizontal displacement of the joints from the geometry of the deflected frame, Fig. 11 (b).

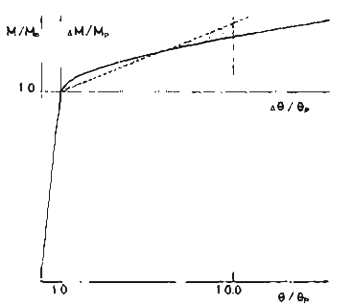

Fig. 13. End Moment-End Slope Relation for Simply-Supported Beam.

After expressing ΔM in terms of $\Delta\theta$ for each member, and then $\Delta\theta$ in terms of the incremental horizontal displacement, we

can find the relation between the incremental load and the incremental horizontal displacement from the equilibrium conditions. The total horizontal displacement equals the sum of this incremental displacement and the displacement at the mechanism state.

As to the unloading process, under constant vertical loads, we assume:

14° The relation between the decrement in the horizontal force and the decrement in the displacement is linear, and is identical with that between the increments for the initial elastic state.

4. Results and Discussion

In Figs. 14 and 15 the relation between the horizontal force H and the displacement Δ is shown. H_p is the collapse load under the horizontal force alone, based on the assumption of perfect plasticity. Δ_1 and Δ_2 are the horizontal displacements of the first and second floors, respectively, Fig. 15 (a). h is the column height. Solid lines refer to the experimental values and dashed lines to the theoretical predictions introduced in the preceding section, the variation of the axial forces being disregarded. The solid circles indicate the formation of plastic hinges. The chain lines refer to the rigid-perfectly plastic theory (see the top of Fig. 14 (a)), and coincide, after the arising of the mechanism state, with the elastic-perfectly plastic theory for the top floor displacement and also approximately for the first floor displacement of two storeyed frames.

Both the experimental and theoretical results show as a general characteristic that the restoring force of a frame is reduced by the vertical loads; the slope of the horizontal force-displacement curve decreases as the displacement increases. A rough agreement is seen between the experiment and the theory which takes care of the strain-hardening effect. In the small deformation range, both indicate linear relations between horizontal force and displacement up to a certain displacement. The theory predicts an appreciably higher slope than the experiment, in particular for the frames with large beam-to-column stiffness ratios (see Figs. 14, 15 and Table 1). The theory has neglected the shearing deformation altogether. Considering the small shear rigidity of a wide flange section and the rather small length-to-depth ratio of the members employed, the shear effect may decrease the slope to a considerable amount. This is estimated approximately in the following way. First, the horizontal force-displacement relation is established by means of the slope-deflection method which takes care of the shearing deformation as well as the bending, the vertical loads being disregarded. It is assumed that the shear force is carried only in the web of a wide flange section, and that the shear stress is distributed uniformly on the web. By comparing the force-displacement relation with that found from the bending deformation alone, we find the deformation due to shear. The shearing deformation is superimposed on the deformation obtained earlier. The thin dotted lines in Figs. 14 and 15 show the slope which takes account of the shear effect. The discrepancy in the initial slope is thus adequately accounted for. The same slope is taken also for the unloading process, showing general agreement with the unloading slope in the experimental curves.

For the inelastic stage of behavior, it is observed that the experimental curves become nearly straight lines, beyond certain displacements (in the deformation

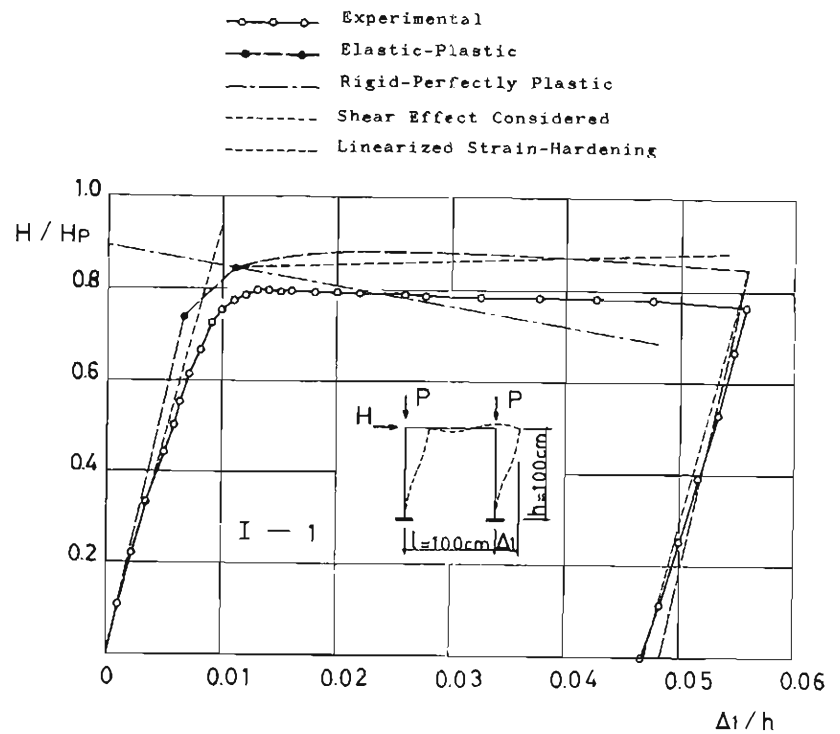

(a) Specimen No. I-1.

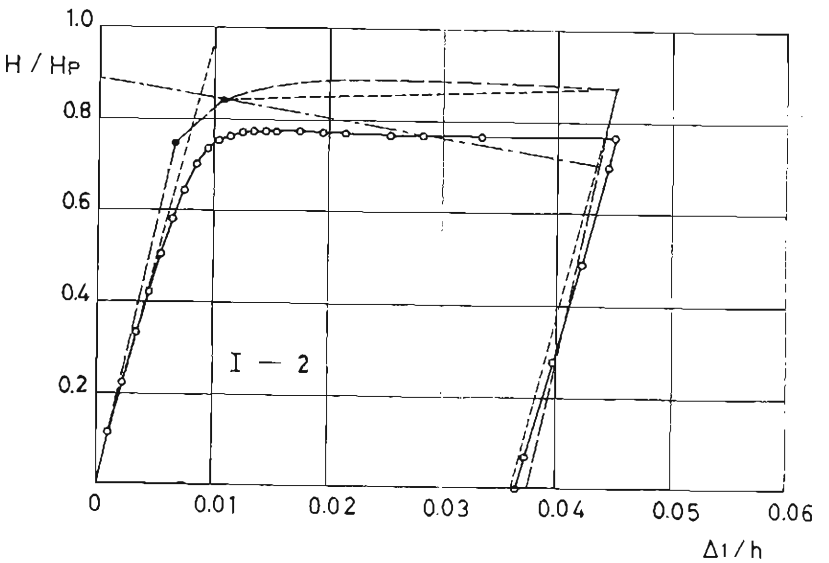

(b) Specimen No. I-2.

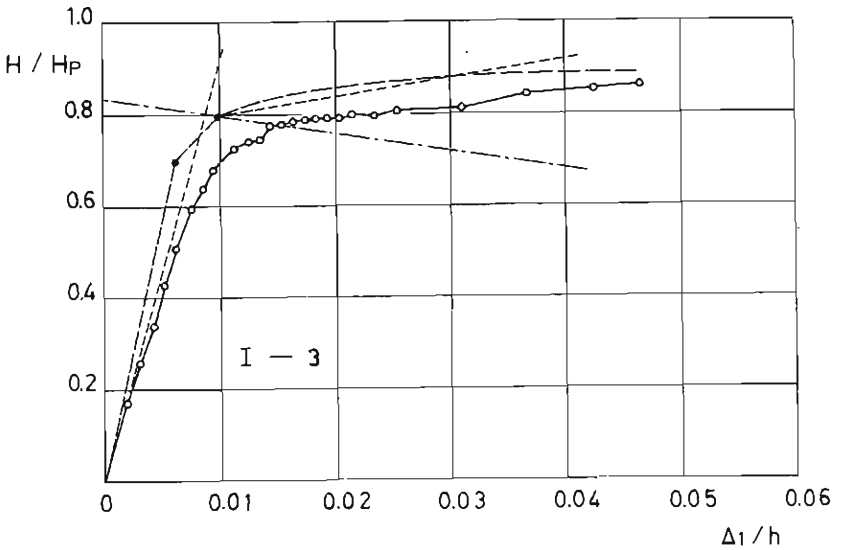

(c) Specimen No. I-3.

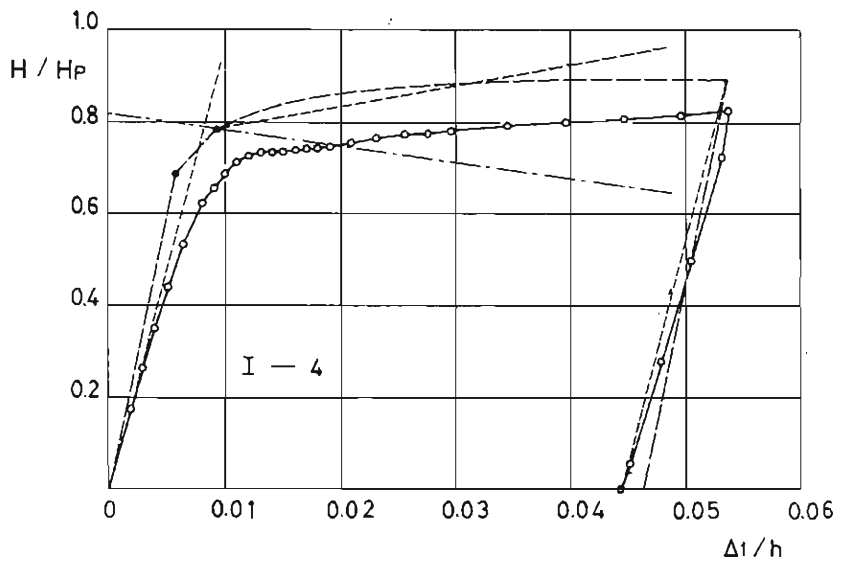

(d) Specimen No. I-4.

Fig. 14. Experimental Results and Theoretical Predictions for One-Storeyed Frames.

range given in this experiment). If we linearize the ΔM-$\Delta\theta$ relation as shown by the thick dotted lines in Fig. 13, then we get straight lines in the strain-hardened range, as shown by thick dotted lines in Figs. 14 and 15. The slope of the linearized ΔM-$\Delta\theta$ relation is determined so as to equate the area under the solid line and that under the solid-dotted line, in the range $0 \leqq \theta/\theta_p \leqq 10$, Fig. 13. It is to be noted that perfect plasticity underestimates the restoring

force by a considerable amount after the arising of the mechanism state and it does not fully describe the frame behavior for a large deformation.

For one-storeyed frames, the theory overestimates the restoring force consistently in the inelastic range, by about 10%. Considering that this is not seen for two-storyed frames, the cause might be concerned with the indeterminancy of the frames but it is not conclusive at this stage of the investigation.

The maximum horizontal force is of main interest. This can be clearly observed in the experiment in the case where the stiffness ratio is small and

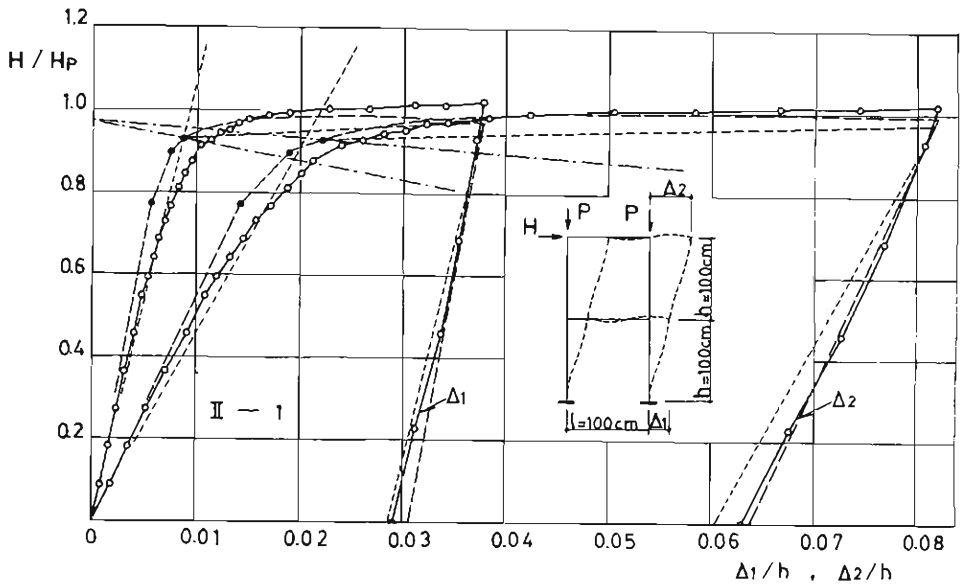

(a) Specimen No. II-1.

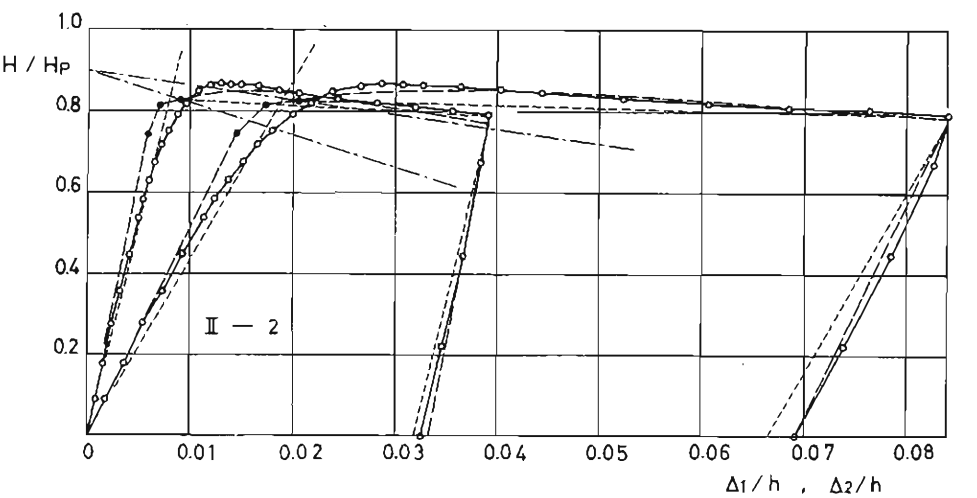

(b) Specimen No. II-2.

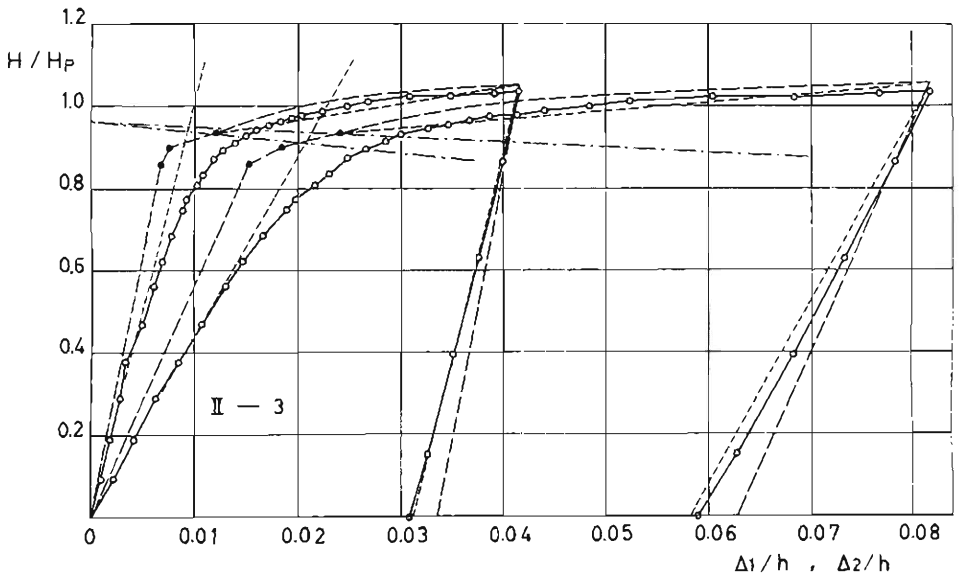

(c) Specimen No. II-3.

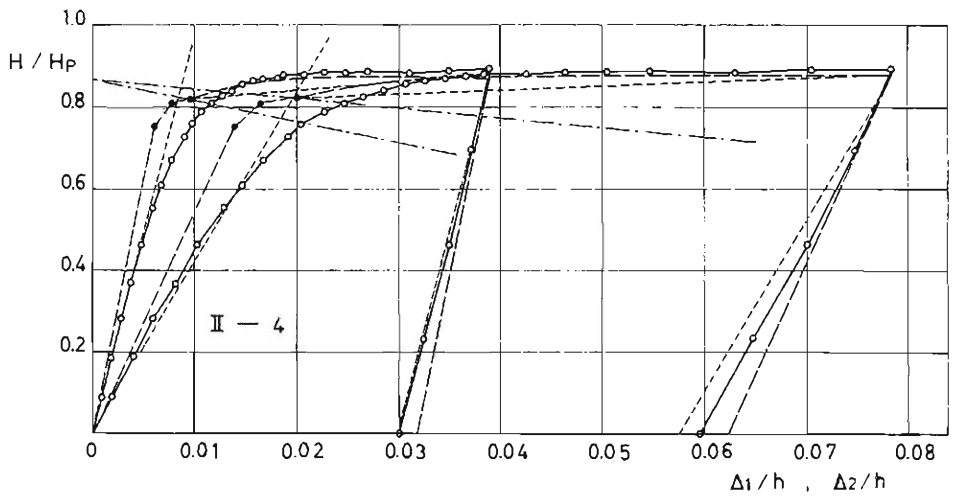

(d) Specimen No. II-4.

Fig. 15. Experimental Results and Theoretical Predictions for Two-Storeyed Frames.

the vertical load is large. This takes place nearly at the displacement of Δ_1/h $=0.010\sim0.015$. This displacement is nearly two times the displacement at which the first theoretical plastic hinge arises in the frame under consideration (see Figs. 14 (a), 14 (b) and 15 (b)). The maximum horizontal force observed (denoted by H_r) is compared with the theoretical horizontal force at the mechanism state (denoted by H_m); the ratio is shown in Table 5. In those cases where the maximum force (corresponding to zero slope in the force-displace-

TABLE 5.
Experimental and Theoretical Results.

Specimen number	Column load			Theoretical predictions for mechanism state									Test results			Ratio
				No column force	Constant column force			Variable column force								
	P (ton)	P/P_y	P/P_c	H_p (ton)	H_m (ton)	Δ_{1m} (cm)	Δ_{2m} (cm)	H'_m (ton)	Δ'_{1m} (cm)	Δ'_{2m} (cm)	Q_{b1} (ton)	Q_{b2} (ton)	$\frac{Q_{b1}+Q_{b2}}{P}$	H_f (ton)	Δ_{1f} (cm)	Δ_{2f} (cm)	H_f/H_m
I—1	20	0.31	0.04	9.34	7.87	1.11		7.88	1.08		3.76		0.19	7.48	1.40		0.95
I—2	20	0.31	0.04	9.24	7.77	1.07		7.80	1.04		3.64		0.18	7.20	1.45		0.93
I—3	20	0.29	0.03	12.25	9.78	0.99		9.62	1.15		5.08		0.25	9.55	1.50		0.98
I—4	20	0.30	0.03	11.70	9.18	0.94		9.10	1.11		4.78		0.24	8.60	1.50		0.94
II—1	10	0.17	0.04	5.63	5.24	0.87	2.21	5.21	0.91	2.27	3.15	3.15	0.61	5.50	1.50	3.35	1.05
II—2	20	0.34	0.07	5.73	4.74	0.89	2.04	4.72	0.76	1.70	3.20	3.20	0.32	5.00	1.30	2.85	1.05
II—3	10	0.17	0.02	8.22	7.64	1.20	2.40	7.43	1.42	2.77	5.90	4.99	1.09	7.70	1.50	3.00	1.01
II—4	20	0.33	0.05	8.38	6.85	0.89	1.99	6.79	1.26	2.48	6.12	4.18	0.52	7.20	1.50	3.05	1.05

P_y : yield load of column
P_c : elastic buckling load of frame
H_p : plastic collapse load of frame
Q_{b1}, Q_{b2} : shear forces of the first and second floor beams at the mechanism state
Subscripts m and f refer to the mechanism state and failure state, respectively.
Primes denote the consideration of the variation in column force.

ment curve) does not appear in the experimental results, the horizontal force at the displacement of $\Delta_1/h=0.015$ is taken to be the appropriate value. Both coincide with an error of within $\pm 7\,\%$. As to the corresponding displacement the experiment shows a larger value than the theory by up to 50 %. The inclusion of the afore-mentioned effect of shearing deformation in the theory would have decreased the difference. The table also includes the horizontal force at the mechanism state from the more elaborate theory which takes into consideration the effect of the variation of the column forces due to the beam shear (denoted by H'_m). The variation affects the horizontal force as little as three percent, at maximum, on the safe or unsafe side. The ratio of the beam shear to the vertical load is shown at the mechanism state, for reference. The fact that the axial force variation has little effect on the restoring force, in spite of a considerable change of the axial force, is because the variation in the column on one side has a favorable effect and that on the other side an unfavorable effect. It is noted, however, that the variation affects the mechanism state displacement by up to 40%.

No difference is observed in frame behavior with specimens either with or without heat treatment.

5. Summary and Conclusions

Models of single bay, one and two story rigid frames were tested, using wide flange sections, from which the characteristic behavior of a multi-story frame was observed. Large vertical loads have induced a significant reduction in the restoring force or unstable character in frame behavior, indicating the impor-

tance of dead loads for the horizontal restoring force in tall buildings.

The elastic-plastic behavior of the frames was reasonably well predicted, until the arising of the mechanism state, by the slope-deflection method taking into consideration the axial forces, when the formation of plastic hinges was considered. The mild steel frames showed more favorable behavior than the theory of perfect plasticity predicts, after the mechanism state was reached. A rough, yet rational, inclusion of the strain-hardening effect in the analysis showed general agreement on the overall behavior of a frame with the experimental results, the closest agreement being found for two-storyed frames.

The restoring force of the frames was not appreciably affected by the variation of the column axial forces due to the beam shear, in the one and two story frames. This result can not be immediately extended, however, to multi-story frames, unless further studies are made on this point, because the variation gets larger as a frame gets higher.

It was observed in this experiment that annealing does not affect overall frame behavior.

Acknowledgment

The results presented in this paper were obtained in the course of research sponsored by Yawata Iron and Steel Co., Ltd. under the supervision of Dr. Y. Yokoo, Professor of Kyoto University. The authors wish to thank Messrs M. Tsuda, I. Mitani and other students of the Department of Architecture, Kyoto University, for invaluable assistance in the preparation of the experiment and the following laborious computations.

Bibliography

1) Wood, R. H., "The Stability of Tall Building," Proc. Inst. Civil Eng., Vol. 11, September 1958, pp. 69–102.
2) Horne, M. R., "The Stability of Elastic-Plastic Structures," Progress in Solid Mechanics, Vol. 2, North Holland Publ. Co., Amsterdam, 1961, pp. 277-322.
3) Horne, M. R. and Merchant, W., "The Stability of Frames," Pergamon Press, Oxford, 1965, pp. 102–153.
4) Ostapenko, A., "Behavior of Unbraced Frames" Lecture Note on Plastic Design of Multi-Story Frames, Chapter 13, Fritz Engineering Laboratory Report No. 273.20, Lehigh University, 1965, pp. 13.1–13.23.
5) Ruzek, J. M., Knudsen, K. E., Johnston, E. R. and Beedle, L. S., "Welded Portal Frames Tested to Collapse," Welding Journal, Vol. 33, No. 9, September 1954 pp. 469-s–480-s.
6) Baker, J. F., Horne, M. R. and Heyman, J., "The Steel Skeleton," Vol. II, Cambridge University Press, Cambridge, 1956, pp. 78–85 and 89–100.
7) Nelson, H. M., Wright, D. T. and Dolphin, J. W., "Demonstrations of Plastic Behavior of Steel Frames," Journal of the Engineering Mechanics Division, EM4, Proc. A. S. C. E., paper No. 1390, October 1957.
8) Baker, J. F. and Charlton, T. M., "A Test on a Two-story Single-bay Portal Structure," British Welding Journal, Vol. 5, No. 5, May 1958, pp. 226–238.
9) Wakabayashi, M., "The Restoring Force Characteristics of Multi-story Frames," Bulletin of the Disaster Prevention Research Institute, Vol. 14, Part 2, February 1965, pp. 29–47.

10) Wakabayashi, M. and Matsui, C., "Study of Elasto-Plastic Stability of Steel Portal Frames Subjected to Vertical and Horizontal Loads," Disaster Prevention Research Institute Annuals, No. 8, March 1965, pp. 127-139 (In Japanese).
11) Makino, M., Sato, T. and Miyazaki, K., "Elasto-Plastic Deformation of Multi-storey Frames under Horizontal Loading," Report of the Building Rerearch Institute Ministry of Construction, Japanese Edition, No. 46, October 1965, pp. 63-78 (In Japanese).
12) Arnold, P., Adams, P. F. and Lu, L. W., "Experimental and Analytical Behavior of a Hybrid Frame," Fritz Engineering Laboratory Report No. 297.18, Lehign University, May 1966.
13) Wakabayashi, M. and Murota, T., "An Experimental Study on the Restoring-Force Characteristics of Tall Frames," Disaster Prevention Research Institute Annuals, No. 9, March 1966, pp. 317-326 (In Japanese).